



^1H , ^{13}C , ^{15}N resonance assignments and secondary structure of yeast oligosaccharyltransferase subunit Ost4 and its functionally important mutant Ost4V23D

Bharat P. Chaudhary¹ · David Zoetewey² · Smita Mohanty¹

Received: 28 January 2020 / Accepted: 16 April 2020 / Published online: 23 April 2020
© Springer Nature B.V. 2020

Abstract

Asparagine-linked glycosylation is an essential and highly conserved protein modification reaction that occurs in the endoplasmic reticulum of cells during protein synthesis at the ribosome. In the central reaction, a pre-assembled high-mannose sugar is transferred from a lipid-linked donor substrate to the side-chain of an asparagine residue in an –N–X–T/S– sequence (where X is any residue except proline). This reaction is carried by a membrane-bound multi-subunit enzyme complex, oligosaccharyltransferase (OST). In humans, genetic defects in OST lead to a group of rare metabolic diseases collectively known as Congenital Disorders of Glycosylation. Certain mutations are lethal for all organisms. In yeast, the OST is composed of nine non-identical protein subunits. The functional enzyme complex contains eight subunits with either Ost3 or Ost6 at any given time. Ost4, an unusually small protein, plays a very important role in the stabilization of the OST complex. It bridges the catalytic subunit Stt3 with Ost3 (or Ost6) in the Stt3–Ost4–Ost3 (or Ost6) sub-complex. Mutation of any residue from M18–I24 in the trans-membrane helix of yeast Ost4 negatively impacts *N*-linked glycosylation and the growth of yeast. Indeed, mutation of valine23 to an aspartate impairs OST function in vivo resulting in a lethal phenotype in yeast. To understand the structural mechanism of Ost4 in the stabilization of the enzyme complex, we have initiated a detailed investigation of Ost4 and its functionally important mutant, Ost4V23D. Here, we report the backbone ^1H , ^{13}C , and ^{15}N resonance assignments for Ost4 and Ost4V23D in dodecylphosphocholine micelles.

Keywords *N*-linked glycosylation · Oligosaccharyltransferase · Solution NMR · Ost4 · Congenital Disorders of Glycosylation · Membrane proteins

Biological context

The oligosaccharyltransferase (OST) enzyme complex is localized next to the ribosome in the endoplasmic reticulum (ER) and carries out the post-translational asparagine-linked or *N*-linked glycosylation in a newly synthesized protein (Kornfeld and Kornfeld 1985). This process is an essential, ubiquitous, and highly conserved protein modification in eukaryotes and some prokaryotes. In the central

step of this reaction, a carbohydrate molecule is covalently attached to the side-chain nitrogen of an asparagine residue in the –N–X–T/S– (X≠P) sequence in a nascent protein (Marshall 1972). *N*-linked glycosylation of proteins is extremely important for many critical biological processes including: protein folding and stability, immune response, protein–protein interactions, protein–ligand interactions, intercellular recognition, and enzyme activities (Helenius and Aebi 2004). Defects in *N*-linked glycosylation results in a series of disorders now known as Congenital Disorders of Glycosylation (CDG). The clinical manifestation of CDG includes: developmental delay, hypoglycemia, dysmorphic features, mental retardation, liver dysfunction, and many others (Freeze 1998; Westphal et al. 2003). In *Saccharomyces cerevisiae*, the OST enzyme complex consists of nine different integral membrane protein subunits. These subunits are further organized into three sub-complexes; sub-complex I [Ost1–Ost5], subcomplex II [Wbp1–Swp1–Ost2]

✉ Smita Mohanty
smita.mohanty@okstate.edu

¹ Department of Chemistry, Oklahoma State University, 74078 Stillwater, OK, USA

² Present Address: Department of Chemistry, Physics and Astronomy, Georgia College and State University, 31061 Milledgeville, GA, USA

and subcomplex III [Stt3–Ost4–Ost3/Ost6] (Karaoglu et al. 1997), where Ost3 and Ost6 are interchangeable homologues. Ost4 in subcomplex III bridges the catalytic subunit Stt3 to the Ost3/Ost6 subunit, maintaining the stability of the subcomplex III and the OST enzyme complex (Kim et al. 2003). Comprehensive mutagenesis studies on Ost4 have shown that substitution of any transmembrane helix residue from 18 to 24 with an ionizable residue impairs the OST activity and negatively impacts the growth of yeast cells (Kim et al. 2000, 2003).

The solution NMR structures of yeast Ost4 (Zubkov et al. 2004), and human Ost4 (Gayen and Kang 2011) have been determined on a chemically synthesized protein in a 4:4:1 chloroform-methanol-water mixed solvent system. The NMR structure of the C-terminal domain of yeast Stt3 in SDS micelles (Huang et al. 2012) and the cryo-EM structure of the whole yeast OST complex in either detergent or in nanodisc have been reported (Bai et al. 2018; Wild et al. 2018). These advances have shed light on the overall structure of the yeast OST complex. However, we still do not know the structural elements that are critical for the stability of the enzyme complex or its function. Correlation of the structure to function of each individual OST subunit is critical to get an insight in to the stabilization of this multimeric enzyme complex, which impacts its function.

We report here the sequence-specific backbone and side-chain assignments of recombinant Ost4 and its critical mutant Ost4V23D solved in dodecylphosphocholine (DPC) micelles.

Methods and experiments

Expression and purification of Ost4 and Ost4V23D

Construction of GB1–OST4 and GB1–OST4V23D plasmids have been reported previously (Chaudhary et al. 2017; Kumar et al. 2012). Ost4 and its critical mutant Ost4V23D were expressed and purified by following previously described methods (Chaudhary et al. 2017; Kumar et al. 2012). Briefly, GB1–Ost4 and GB1–Ost4V23D were transformed in *E. coli* BL21DE3pLysS cells (Stratagene). The overnight culture of each expression was diluted to an OD₆₀₀ of 0.06 using fresh M9 media supplemented with 4 g/L ¹³C-glucose, 1.2 g/L ¹⁵N–NH₄Cl, 1 mg/L thiamine, 100 µg/mL ampicillin 2 mM MgSO₄, 50 µM CaCl₂, and 100 µM trace elements. The culture was then incubated at 37 °C until OD₆₀₀ reached between 0.4 and 0.6. Expression was induced at 30 °C by addition of 1 mM isopropyl-β-D-thiogalactopyranoside (IPTG). After 8 h, the cells were harvested by centrifugation at 9000 rpm. The cells were resuspended in lysis buffer (50 mM sodium phosphate buffer, pH 7.4, 200 mM sodium chloride, 0.01% sodium azide) and

then sonicated to lyse the cells. After lysis by sonication, the supernatant liquid was loaded onto a pre-equilibrated Ni–NTA column for purification taking advantage of the C-terminal 6×His-tag. The proteins were eluted under the flow of gravity. After removal of the GB1 tag from the protein by thrombin cleavage, the C-terminal 6×His-tagged proteins were checked for purity by SDS-PAGE followed by reconstitution in 100 mM deuterated DPC micelles for NMR data collection.

NMR experiments

All NMR data were collected using either a Bruker Avance II 800 MHz spectrometer equipped with a 5 mm triple resonance pulsed-field gradient TCI cryoprobe at National High Field Magnetic Laboratory, Tallahassee, Florida, or Varian Inova 600 MHz or 900 MHz spectrometers equipped with cold probes at the Department of Pharmacology, University of Colorado School of Medicine, Colorado, or a Bruker Avance III 600 MHz or a Varian Inova 900 MHz spectrometers with cryoprobes at the University of Minnesota NMR center. For backbone and side-chain assignments of Ost4 and Ost4V23D, the following NMR experiments were performed: 2D {¹H, ¹⁵N} HSQC, 2D {¹H, ¹³C} HSQC, 3D HNCACB, 3D CBCACONH, 3D HNCA, 3D HN(CO)CA, 3D HNHAHB, 3D HBHA(CO)NH, 3D ¹³C-edited HCCH-TOCSY, 3D H(CCO)NH-TOCSY, and 3D ¹⁵N-edited HSQC-TOCSY experiments were performed. All spectra were acquired at 308 K in NMR buffer containing 50 mM phosphate buffer (pH 6.5), 1 mM EDTA, 0.5% NaN₃, 100 mM deuterated DPC, and 5% D₂O. Assignments were confirmed using 3D ¹⁵N-edited NOESY-HSQC spectra with mixing times of 90 ms and 120 ms. All the spectra were processed using NMRPipe (Delaglio et al. 1995) and analyzed by using NMRFAM-SPARKY (Lee et al. 2015).

Resonance assignments and data deposition

Figure 1 shows the overlay of 2D {¹H, ¹⁵N} HSQC spectra of Ost4 and Ost4V23D with resonance assignments. Well-resolved resonances in 2D {¹H, ¹⁵N} HSQC of both the proteins indicate that the proteins are well-folded in 100 mM DPC micelles.

The assignments for Ost4 and Ost4V23D were carried out independently with triple resonance NMR data sets that were acquired separately for each protein. The ¹H, ¹⁵N, and ¹³C resonance assignments for Ost4 and Ost4V23D have been deposited into BMRB (<http://www.bmrb.wisc.edu>) with accession number 50159 and 50160 respectively. Each recombinant protein is composed of 45 residues including nine additional residues in the C-terminus (Fig. 2). Besides the 6×His-tag (H40–H45), both the proteins contain three additional residues: R37, L38, and E39.

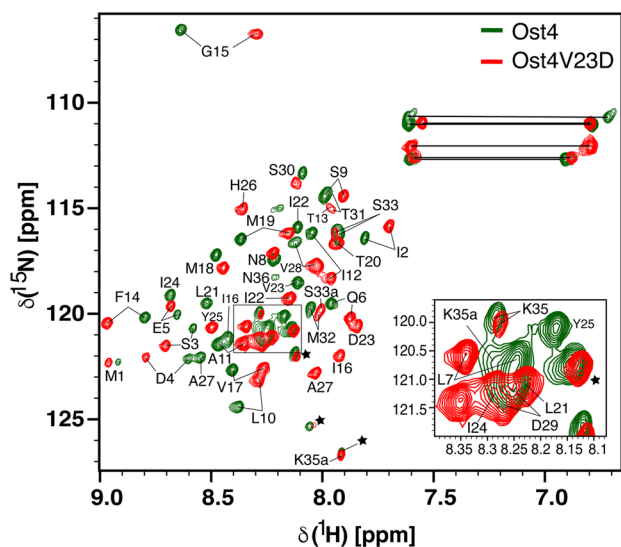


Fig. 1 Overlay of 2D $\{^1\text{H}, ^{15}\text{N}\}$ HSQC spectra of Ost4 (green) with Ost4V23D (red) at pH 6.5 at 308 K. These spectra were collected under identical conditions. The proteins contain 45 amino acid residues including nine additional residues in the C-terminal 6xHis-tag. Only the terminal histidine (H45) of the hexa-histidine tag was assigned. The residues from M1 to N36 belong to Ost4 and Ost4V23D. The residues that do not belong to the proteins are: R37, L38, E39, and H40-H45 in the C-terminus. The residues indicated by * in the spectrum are from the tag. Resonances of the side-chain of glutamine and asparagine amide groups are not labeled. An expanded view of the central region of the HSQC spectrum is shown on the lower right corner of the spectrum

The assignment of backbone resonances (^1H , ^{15}N , $^{13}\text{C}_\alpha$, and $^{13}\text{C}_\beta$) of Ost4 was completed for all residues except ^1H and ^{15}N of T13, T20, and H26 in addition to C_β for I12 in the primary sequence (M1–N36). In Ost4V23D, backbone resonance (^1H , ^{15}N , $^{13}\text{C}_\alpha$, and C_β) assignments were completed for all residues except ^1H , ^{15}N , $^{13}\text{C}_\alpha$ of T13 in the primary sequence (M1–N36). The backbone and side-chain

resonance assignments were completed for 95% and 91% respectively for Ost4 and 98% and 87.6% for Ost4V23D. The lone proline residue at position 34 is present in cis and trans forms for both of the proteins. Thus, two sets of resonances for residues S33 and K35 were observed for Ost4 and Ost4V23D in the 2D $\{^1\text{H}, ^{15}\text{N}\}$ HSQC spectra.

The secondary structures of Ost4 and Ost4V23D were determined independently using chemical shifts in TALOS+ (Shen et al. 2009) and SSP (Marsh et al. 2006). As shown in Fig. 2, both programs predict a single helix encompassing residues D4–M32 for Ost4 and Ost4V23D. In addition, single residue-specific secondary structure propensity (SSP) scores were calculated for both the proteins separately by using their $^{13}\text{C}_\alpha$ and $^{13}\text{C}_\beta$ chemical shifts (Fig. 3). The SSP scores shown in Fig. 3 illustrate the difference in secondary structure propensities between Ost4 and Ost4V23D proteins more prominently than the $\Delta\delta\text{C}_\alpha$ and $\Delta\delta\text{C}_\alpha - \Delta\delta\text{C}_\beta$ plots shown in Fig. 2. On the basis of the SSP scores, the overall propensities for α -structure of Ost4 and Ost4V23D are ~47% and ~60% respectively. This observation is consistent with what we have reported previously (30% and 62% helicity for Ost4 and Ost4V23D respectively) using circular dichroism (Chaudhary et al. 2017). Since Ost4 and Ost4V23D have significantly different α -structure propensity, their 2D $\{^1\text{H}, ^{15}\text{N}\}$ HSQC spectra are distinct (Fig. 1).

The distinct 2D $\{^1\text{H}, ^{15}\text{N}\}$ HSQC spectra of Ost4 and Ost4V23D along with significant differences in their helical structure propensity suggest that mutation of V23 to D changes the environment around the protein, thus affecting the stability and function of the OST enzyme. The studies performed in this work represent important steps towards understanding the function of yeast OST at the molecular level. Structure–function studies of OST enzyme complex are critical in elucidating the mechanism of *N*-linked glycosylation. The 3D structure determination of Ost4 and Ost4V23D is in progress by high-resolution solution NMR.

Fig. 2 TALOS+ predicted secondary structure, $\Delta\delta C_\alpha$ – $\Delta\delta C_\beta$, and $\Delta\delta C_\alpha$ secondary chemical shifts: **a** Ost4 and **b** Ost4V23D. Positive values in secondary chemical shifts indicate α -structure propensity and negative values indicate β -structure or random coil propensity. The secondary chemical shifts were derived by using SSP program (Marsh et al. 2006). The residue D23 (highlighted in purple) is the mutated residue in Ost4V23D. The residues R37, L38, and E39 (highlighted in yellow) along with the C-terminal 6 \times His-tag tag (highlighted in red) do not belong to Ost4 or Ost4V23D

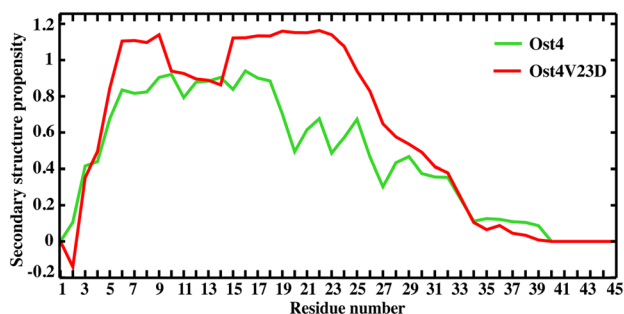
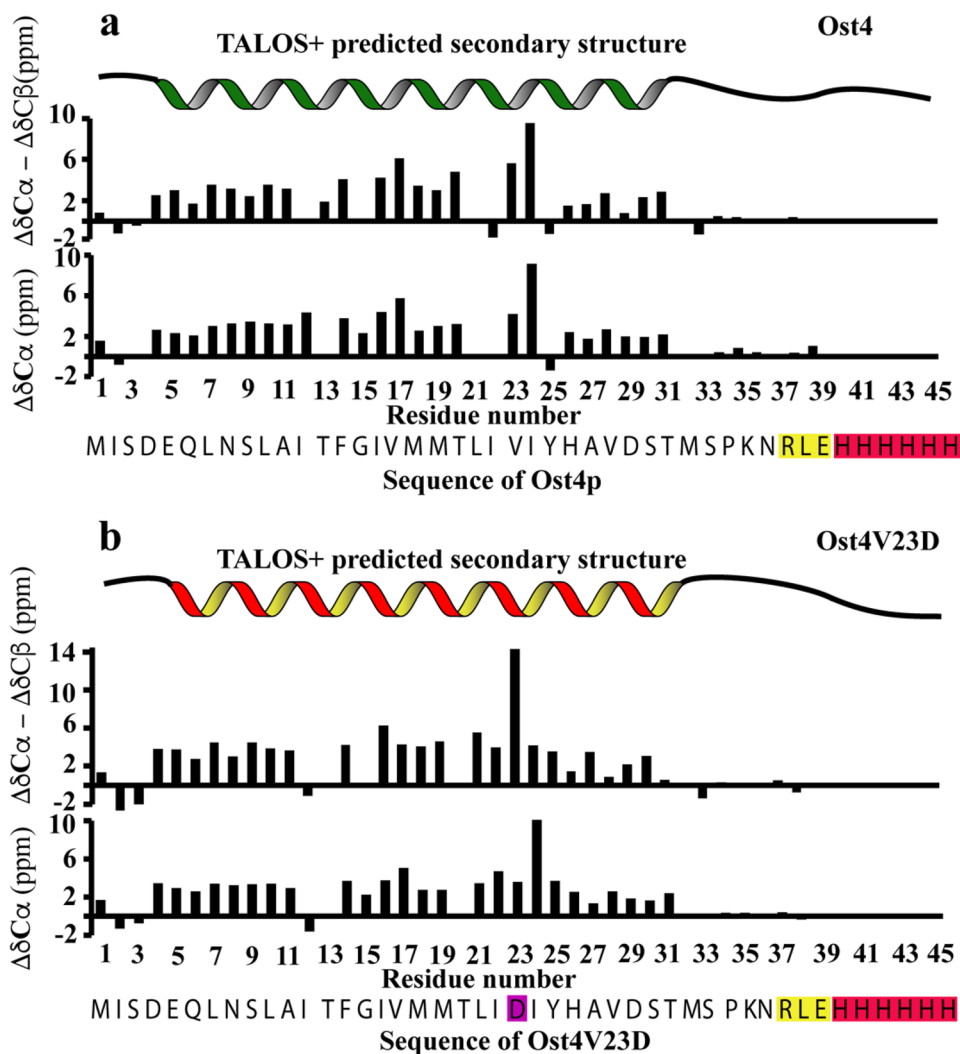


Fig. 3 Secondary structure propensities for wildtype Ost4 (green line) and mutant Ost4V23D (red line). The SSP for each protein were calculated using $^{13}C_\alpha$ and $^{13}C_\beta$ chemical shifts with SSP limit of 1.2. Ost4V23D mutant protein contains higher overall α -structural propensity than that of wildtype Ost4

Acknowledgements This work was financially supported by National Science Foundation Award CHE-1807722 and DBI-1726397 to SM. A portion of this work was performed at the National High Magnetic Field Laboratory, Tallahassee, FL, which is supported by NSF

Cooperative Agreement No. DMR-1644779 and the State of Florida. We thank Dr. Chengdong Huang for recording some of the Ost4 NMR data for us. We thank Dr. Thomas Webb of Auburn University, Auburn, AL for the critical reading of the manuscript. We thank Ms. Ishani Ray for help with proofreading of the manuscript.

Author Contributions SM conceived, designed the strategies and techniques employed, supervised the research, and analyzed the data. BC expressed, purified and reconstituted both recombinant proteins, performed all NMR experiments, and processed NMR data. BC and DZ analyzed and completed the backbone and side-chain resonance assignments. SM and BC wrote the paper and BC prepared the figures.

Compliance with ethical standards

Conflict of interest The authors declare that they have no conflict of interest with the contents of this article.

References

- Bai L, Wang T, Zhao G, Kovach A, Li H (2018) The atomic structure of a eukaryotic oligosaccharyltransferase complex. *Nature* 555:328–333. doi:<https://doi.org/10.1038/nature25755>
- Chaudhary B, Mazumder S, Mohanty S (2017) Production and biophysical characterization of a mini-membrane protein, Ost4V23D: A functionally important mutant of yeast oligosaccharyltransferase subunit Ost4p. *Protein Expr Purif* 139:43–48. doi:<https://doi.org/10.1016/j.pep.2017.07.009>
- Delaglio F, Grzesiek S, Vuister GW, Zhu G, Pfeifer J, Bax A (1995) NMRPipe: a multidimensional spectral processing system based on UNIX pipes. *J Biomol NMR* 6:277–293
- Freeze HH (1998) Disorders in protein glycosylation and potential therapy: Tip of an iceberg? *J Pediatr* 133:593–600. doi:[https://doi.org/10.1016/S0022-3476\(98\)70096-4](https://doi.org/10.1016/S0022-3476(98)70096-4)
- Gayen S, Kang C (2011) Solution structure of a human minimembrane protein Ost4, a subunit of the oligosaccharyltransferase complex. *Biochem Biophys Res Commun* 409:572–576. doi:<https://doi.org/10.1016/j.bbrc.2011.05.050>
- Helenius A, Aebi M (2004) Roles of N-linked glycans in the endoplasmic reticulum. *Annu Rev Biochem* 73:1019–1049. doi:<https://doi.org/10.1146/annurev.biochem.73.011303.073752>
- Huang C, Bhaskaran R, Mohanty S (2012) Eukaryotic N-glycosylation occurs via the membrane-anchored C-terminal domain of the Stt3p subunit of oligosaccharyltransferase. *J Biol Chem* 287:32450–32458. doi:<https://doi.org/10.1074/jbc.M112.342253>
- Karaoglu D, Kelleher DJ, Gilmore R (1997) The highly conserved Stt3 protein is a subunit of the yeast oligosaccharyltransferase and forms a subcomplex with Ost3p and Ost4p. *J Biol Chem* 272:32513–32520
- Kim H, Park H, Montalvo L, Lennarz WJ (2000) Studies on the role of the hydrophobic domain of Ost4p in interactions with other subunits of yeast oligosaccharyl transferase. *Proc Natl Acad Sci USA* 97:1516–1520. <https://doi.org/10.1073/pnas.040556797>
- Kim H, Yan Q, Von Heijne G, Caputo GA, Lennarz WJ (2003) Determination of the membrane topology of Ost4p and its subunit interactions in the oligosaccharyltransferase complex in *Saccharomyces cerevisiae*. *Proc Natl Acad Sci USA* 100:7460–7464. <https://doi.org/10.1073/pnas.1332735100>
- Kornfeld R, Kornfeld S (1985) Assembly of asparagine-linked oligosaccharides. *Annu Rev Biochem* 54:631–664. doi:<https://doi.org/10.1146/annurev.bi.54.070185.003215>
- Kumar A, Ward P, Katre UV, Mohanty S (2012) A novel and simple method of production and biophysical characterization of a mini-membrane protein, Ost4p: a subunit of yeast oligosaccharyl transferase. *Biopolymers* 97:499–507. doi:<https://doi.org/10.1002/bip.22028>
- Lee W, Tonelli M, Markley JL (2015) NMRFAM-SPARKY: enhanced software for biomolecular NMR spectroscopy. *Bioinformatics* 31:1325–1327. doi:<https://doi.org/10.1093/bioinformatics/btu830>
- Marsh JA, Singh VK, Jia Z, Forman-Kay JD (2006) Sensitivity of secondary structure propensities to sequence differences between alpha- and gamma-synuclein: implications for fibrillation. *Prot Sci* 15:2795–2804
- Marshall RD (1972) Glycoproteins. *Annu Rev Biochem* 41:673–702. <https://doi.org/10.1146/annurev.bi.41.070172.003325>
- Shen Y, Delaglio F, Cornilescu G, Bax A (2009) TALOS+: a hybrid method for predicting protein backbone torsion angles from NMR chemical shifts. *J Biomol NMR* 44:213–223. doi:<https://doi.org/10.1007/s10858-009-9333-z>
- Westphal V, Xiao M, Kwok PY, Freeze HH (2003) Identification of a frequent variant in ALG6, the cause of Congenital Disorder of Glycosylation-Ic. *Hum Mutat* 22:420–421. doi:<https://doi.org/10.1002/humu.9195>
- Wild R, Kowal J, Eyring J, Ngwa EM, Aebi M, Locher KP (2018) Structure of the yeast oligosaccharyltransferase complex gives insight into eukaryotic N-glycosylation. *Science* 359:545–550. <https://doi.org/10.1126/science.aar5140>
- Zubkov S, Lennarz WJ, Mohanty S (2004) Structural basis for the function of a minimembrane protein subunit of yeast oligosaccharyltransferase. *Proc Natl Acad Sci USA* 101:3821–3826. <https://doi.org/10.1073/pnas.0400512101>

Publisher's Note Springer Nature remains neutral with regard to jurisdictional claims in published maps and institutional affiliations.